



Title:

Assessing the Planarity of Bruch's Membrane Opening

Authors:

John K. Johnstone, jkj@uab.edu, Computer Science, The University of Alabama at Birmingham

Keywords:

Optic nerve head morphometry, measurement of planarity.

DOI: 10.14733/cadconfP.2026.60-64

Introduction

Since Bruch's membrane opening, a structure in the optic nerve head, is almost planar, its best-fitting plane is often used to define a reference plane for morphometry of the optic nerve head [6]. This leads to a natural question: how planar is Bruch's membrane opening?

By applying classical CAD machinery (plane fitting, intersection, dimension reduction), this paper proposes a tool for assessing the planarity of Bruch's membrane opening. This tool could be used by clinicians to aid understanding of the robustness of measurements that use a reference plane defined by Bruch's membrane opening; and more promisingly, as a new statistic for analysis of the optic nerve head. The contribution of the paper is the suggestion of this new tool for ONH morphometry, and the choice of tools from CAD machinery to be used in the development of this new tool.

The structure of the paper is as follows. The importance of Bruch's membrane opening as a reference structure in morphometry of the optic nerve head is explained. An algorithm to build a point cloud of Bruch's membrane opening is developed. Then, after reviewing a classical algorithm to compute the best-fitting plane of a point cloud, an algorithm to assess the planarity of Bruch's membrane opening is proposed. We finish with conclusions and directions for future work.

Bruch's membrane opening

One of the visible structures in optical coherence tomography (OCT) images of the optic nerve head (ONH) is Bruch's membrane (Fig. 1). Bruch's membrane opening (BMO) is the inner boundary of Bruch's membrane at the anterior end of the neural canal. Since Bruch's membrane opening tends to be almost planar, its best-fitting plane (the **Bruch plane**) is commonly used as a reference plane for morphometry of the optic nerve head. Since the development of certain optic neuropathies is associated with structural changes in the optic nerve head, measurement of the optic nerve head (ONH morphometry) is used to better understand these neuropathies. For example, measurements include the depth and volume of two anatomical structures, the inner limiting membrane and the anterior lamina, below the Bruch plane. As intra-ocular pressure builds up and ONH morphology deforms, these depths and volumes may increase.

Bruch's membrane is gathered from an ONH dataset, as follows. An OCT volume of the optic nerve head is imaged in a clinical setting. The OCT volume is then sliced into a series of OCT images, by planes that rotate around an axis that passes through the neural canal. The planar slicing simplifies segmentation, since the segmentation is now from a 2d image rather than a 3d volume. The rotational

structure of the slices concentrates data in the neural canal, as opposed to a conventional parallel set of planes as in CT. The OCT images are then segmented by hand into categories, such as the inner limiting membrane, Bruch’s membrane, anterior sclera, and anterior lamina (Fig. 1). This yields a point cloud of the optic nerve head organized into categories and slices, called an **ONH dataset** [7].

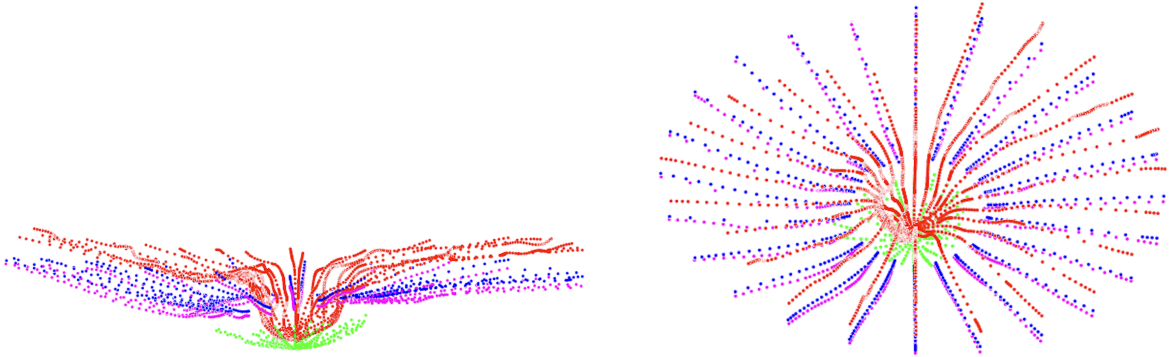


Fig. 1: An ONH dataset with four categories. Left: The categories: inner limiting membrane (red), Bruch’s membrane (blue), anterior sclera (magenta), and anterior lamina (green) Right: A different viewpoint of this dataset, showing its organization into radial slices.

Building the point cloud of Bruch’s membrane opening

This section develops an algorithm to build the point cloud of Bruch’s membrane opening from an ONH dataset. Bruch’s membrane (blue in Fig. 1) does not cross the neural canal, and where it stops defines Bruch’s membrane opening (the black samples of Fig. 2). Bruch’s membrane opening is isolated using the axis of rotation of the planar slices, as follows.

The OCT images, and therefore also the slices, rotate around an axis that passes through the neural canal of the optic nerve head (Fig. 1 and 2). Bruch’s membrane opening is isolated by identifying the samples of Bruch’s membrane that are closest to the axis of rotation, since the axis of rotation passes through the neural canal. This subtler approach is necessitated by the fact that the samples of Bruch’s membrane are not necessarily ordered consistently in the ONH dataset; for example, the BMO sample need not always be the first sample of a BM slice. Therefore, the first step in extracting the BMO cloud is to find the axis of rotation of the ONH dataset.

Consider an algorithm to find the axis of rotation of an ONH dataset. Since each slice plane contains the axis of rotation, the axis of rotation may be found by the intersection of any two slice planes. And since each category slice lies in a plane, a slice plane may be found as the best-fitting plane of its associated slice cloud. Though in theory any noncollinear triple of points would define the plane, the best-fitting plane is a more robust approach to extracting the plane. The next section develops a robust algorithm for the best-fitting plane of a point cloud.

Which category should be used to define the slice planes? We choose the inner limiting membrane (**ILM**) for two reasons. First, ILM is guaranteed to be present in the dataset, since it is always visible in OCT images and since important measurements depend on it, such as cup depth. Second, ILM is typically the most densely sampled category, for the same reasons. Therefore, the axis of rotation is found as the intersection of the best-fitting planes of the two ILM slices with the most points.

Consider a robust algorithm to compute the intersection of two planes. Let the two planes be defined by the normals N_i and the points P_i ($i = 1, 2$). Since a plane with point P and normal N is defined by

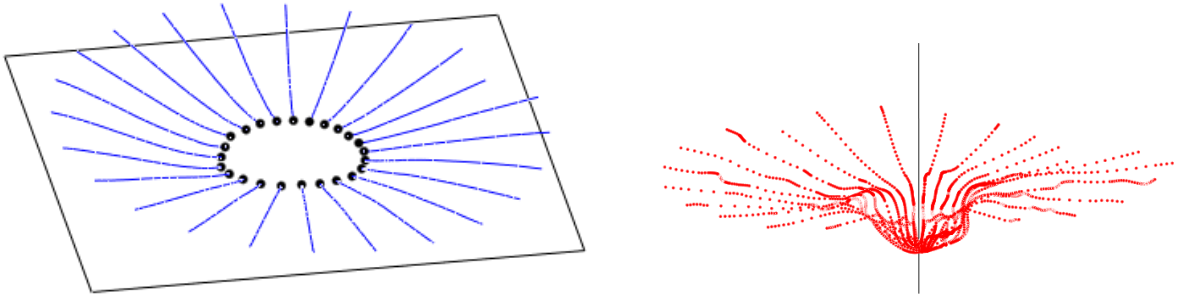


Fig. 2: Left: Bruch's membrane (blue), Bruch's membrane opening (black), and the best-fitting plane of Bruch's membrane opening (the Bruch plane). Right: The axis of rotation of the radial slices.

the equation $(X - P) \cdot N = 0$, a point on the intersection can be found by solving the underdetermined linear system built from the two equations $X \cdot N_1 = P_1 \cdot N_1$ and $X \cdot N_2 = P_2 \cdot N_2$. This rectangular system is solved using QR decomposition. The system has an infinite number of solutions: a good solution can be found using a C++ method like Eigen's `colPivHouseholderQr.solve` [1]. The direction vector of the line of intersection is the cross product of the plane normals.

An algorithm to find the axis of rotation is in Algorithm 1 and an algorithm to extract Bruch's membrane opening is in Algorithm 2.

Algorithm 1 Finding the axis of rotation of an ONH dataset

- 1: Find the two ILM slices with the most points.
 - 2: Find the best-fitting plane of each of these point clouds.
 - 3: Find the intersection of these two planes, which is the axis of rotation.
-

Algorithm 2 Extracting the point cloud of Bruch's membrane opening

- 1: Find the axis of rotation.
 - 2: Define the BMO point cloud by extracting the samples of the BM slices closest to the axis of rotation.
-

Computing the best fitting plane

We now review an algorithm to find the best-fitting plane of a point cloud $\{p_i\}_{i=1}^n$. We choose to use a classical algorithm based on PCA [4] from SVD [3]. Since there are no outliers present in our point clouds, a RANSAC approach [2] is not required. This algorithm is used to compute the Bruch reference plane from the BMO cloud, as well as to compute the axis of rotation.

By best-fitting plane, we mean best-fitting in the least squares sense: the plane P that minimizes the sum of the squared distances of the points of the cloud from the plane:

$$P = \operatorname{argmin}_P \sum_{i=1}^n \operatorname{dist}^2(p_i, P) \quad (2.1)$$

A point on the best-fitting plane is simply the mean μ of the point cloud. However, finding the normal of the best-fitting plane requires principal component analysis (**PCA**) of the cloud. The normal of the best-fitting plane is the shortest principal component, the vector v that minimizes the variance of the orthogonal projection of the cloud onto v :

$$N = \operatorname{argmin}_v \operatorname{Var}(\operatorname{proj}_v(\{p_i\})) \quad (2.2)$$

PCA can use either spectral analysis or singular value decomposition (SVD), but SVD typically yields better results.

The algorithm to find the normal of the best-fitting plane of the point cloud X , using SVD-based PCA, is in Algorithm 3. The point cloud is stored in a column-major data matrix X : the i th point is the i th column of X . This allows vectorized computation. Let the size of the point cloud be n .

Algorithm 3 Finding the normal of the best-fitting plane of a point cloud

- 1: Find the sample mean μ of the cloud.
This can be done using the vectorized mean of each row of X .
 - 2: Mean normalize the cloud, by subtracting μ from each point.
This can be done in a vectorized computation on each column of X , yielding the data matrix \bar{X} .
 - 3: Build the sample covariance matrix C of the mean-normalized cloud.
This can be done using a single matrix multiplication: $C = \frac{1}{n} \bar{X} \bar{X}^t$.
 - 4: Compute the singular value decomposition $C = U \Sigma V^t$ of the covariance matrix C .
 - 5: The last column of U is the normal of the best-fitting plane of X .
-

In the SVD of the covariance matrix (step 4), the columns of U are the principal component directions of the cloud. These columns are sorted in nonincreasing order of axis length. Since the axis length (encoded in the singular values) is correlated with the variance of the cloud's projection on the principal component, the shortest principal component is the last column of U . That is, the normal of the best-fitting plane is the last column of U . The C++/Eigen code for the computation of the best-fitting plane is but 4 lines long, since Eigen [1] allows efficient and robust vectorized computation.

Assessing the planarity of Bruch's membrane opening

We may now finally address the question of assessing the planarity of the BMO, by developing a robust measure of the planarity of a point cloud. An obvious measure is the maximal distance of a point of Bruch's membrane opening from its best-fitting plane, normalized by the radius of the BMO cloud. However, we prefer a more subtle and robust measure, variance lost.

Consider the orthogonal projection of the BMO cloud onto its best-fitting plane. This dimension reduction, replacing a cloud in 3-space by a cloud in 2-space, is a well studied problem [5]. The information lost by this dimension reduction is measured by the variance lost. This is effectively the information lost by considering the cloud to be planar. Let $\{\sigma_i\}$ be the singular values of the SVD of the covariance matrix of the mean-normalized point cloud, in non-increasing order. These singular values are already available from the principal component analysis that found the best-fitting plane (Step 4 of Algorithm 3). The

variance lost by reducing a cloud in d -space to a cloud in k -space, by projecting onto the space spanned by its top k principal components, is:

$$1 - \frac{\sum_{i=1}^k \sigma_i}{\sum_{i=1}^d \sigma_i} = \frac{\sum_{i=k+1}^d \sigma_i}{\sum_{i=1}^d \sigma_i} \quad (2.3)$$

Therefore, the variance lost by reducing a BMO cloud in 3-space to its best-fitting plane is:

$$\frac{\sigma_3}{\sigma_1 + \sigma_2 + \sigma_3} \quad (2.4)$$

That is, the normalized last singular value is an indication of how much the point cloud differs from a plane, or how much information is lost in treating it as planar. (2.4) is our proposed planarity measure, with 0 indicating perfect planarity. It is a scale-invariant measure, as desired by this problem. This may become a new feature or statistic for an ONH dataset, allowing it to be compared against other datasets.

Conclusions and future work:

Since Bruch's membrane opening influences morphometry of the optic nerve head, such as downstream computations of cup depth and laminar depth, a deeper understanding of its structure is valuable. This paper has proposed a new statistic (2.4) to measure BMO planarity. Robust vectorizable algorithms were chosen to compute this statistic from an ONH dataset: using SVD for PCA, using variance lost for assessing planarity, using column-major data matrices, using the best-fitting plane to find the plane of a slice, and using Householder QR decomposition for finding a point on the axis of rotation.

A natural question to ask next is: how elliptical is Bruch's membrane opening? Bruch's membrane opening is not only close to planar but close to elliptical (Figure 2) and its best-fitting ellipse is used as a reference ellipse for morphometry, such as defining an elliptical cylinder to bound volumes. Another problem for future study is the planarity and ellipsoidality of the anterior lamina, another important category in the optic nerve head.

References:

- [1] Eigen: <https://eigen.tuxfamily.org>
- [2] Fischler, M., Bolles, R.: Random Sample Consensus: A Paradigm for Model Fitting with Applications to Image Analysis and Automated Cartography, *Communications of the ACM*, 24(6), 1981, 381–395. <https://doi.org/10.1145/358669.358692>
- [3] Golub, G., Van Loan, C.: *Matrix Computations*, The Johns Hopkins University Press (4th ed), 2013. <https://doi.org/10.56021/9781421407944>
- [4] Hartley, J., Zisserman, A.: *Multiple View Geometry*, Cambridge University Press (2nd ed), 2004. <https://doi.org/10.1017/CB09780511811685>
- [5] Jolliffe, I.: *Principal Component Analysis*, Springer, 2002. <https://doi.org/10.1007/b98835>
- [6] Johnstone, J., Fazio, M., Rojananuangnit, K., Smith, B., Clark, M., Downs, J.C., Owsley, C., Girard, M., Mari, J.-M., Girkin, C.: Variation of the Axial Location of Bruch's Membrane Opening with Age, Choroidal Thickness and Race, *Investigative Ophthalmology and Visual Science*, 55(3), 2014, 2004-2009. <https://doi.org/10.1167/iovs.13-12937>
- [7] Johnstone, J.: Storing Optic Nerve Head Geometry in a Category-Major PLY format, *Computer-Aided Design and Applications*, 22(4), 2025, 555-565. <https://doi.org/10.14733/cadaps.2025.555-565>